Transition to rivulets in a highly sheared liquid film on an airfoil

Anne Gosset[1], Daniel Rodríguez Calvete[1], Philippe Villedieu[2]
[1] *University of A Coruña, Department of Naval and Oceanic Engineering, Ferrol, Spain*
[2] *ONERA, DMAE, Toulouse, France*
Corresponding author: anne.gosset@udc.es

Keywords: sheared film flow, rivulets, icing

1. Introduction and background

This work deals with the prediction of the breakup of a sheared liquid film into rivulets. It is motivated by the needs of the aeronautic industry, for the study of the icing of aircraft components. When an aircraft flies through icing clouds or rain, supercooled water droplets impinge on its wings and form ice if these aerodynamic surfaces are not thermally protected. Usual anti-icing systems involve heating the leading edge of the airfoil. As they are unable to freeze, the droplets tend to coalesce and form a continuous thin water film. This runback water flows to downstream regions, driven by pressure and shear forces due to the external airflow around the airfoil, and its thickness varies streamwise. When a critical thickness is reached, surface tension effects become dominant, and it is energetically favorable for the film flow to break up into rivulets. The presence of rivulets affects the performance of the anti-ice system because it decreases the effective area of heat and mass transfer between the water, the airfoil surface, and the external airflow.
It is therefore fundamental to be able to predict where the water film will break up into rivulets on an airfoil, and which rivulet pattern will be adopted. This can be tackled through different approaches: the film flow and rivulets can be fully computed, taking into account the contact angle force in the lubrication equations, and studying the stability of the contact line, e.g. [1]. But this approach is time consuming, and a macroscopic approach is usually preferred in ice accretion / anti-icing codes. In this type of approach, a wetness factor is computed and there is no explicite calculation of the rivulets. Al-Khalil et al. [2] and Lima da Silva et al. [3] have used the Minimum Total Energy (MTE) criteria to predict transition to rivulets in their respective codes. This criteria allows determining if there will be transition or not to rivulets. For that, at film breakdown, the mechanical total energy (kinetic+surface tension) and mass are conserved from continuous film to rivulet flow. Then the most stable rivulet configuration is found by minimizing the total energy. The MTE approach has been extensively validated for falling films e.g. [1], but almost never for sheared films because of the lack of experimental data. In addition, the MTE modeling of rivulets in anti-icing codes has never been validated in isothermal conditions.
In this work, the MTE model is implemented for an isothermal water film flow on a NACA0012 profile. One input of the MTE model in the case of a sheared film is the distribution of shear stress. Here it is computed over the airfoil through single phase computations of the airflow, assuming that the presence of the liquid film does not affect the shear stress. The critical film thickness h_0 and the optimum spacing between rivulets λ are computed along the airfoil, and these predictions are compared to the experimental measurements of Zhang et al. [4] who provide a complete mapping of the water film thickness on a NACA0012 profile subject to shear flow. In their tests, the water film is generated by two sprays impinging in the leading edge area of the foil at zero angle of attack, and the airflow speed is varied between 10 and 25 m/s, corresponding to Reynolds numbers $Re_c = 0.67 \cdot 10^5 - 1.69 \cdot 10^5$.

2. Minimum Total Energy model

The Minimum Total Energy model (MTE) was initiated by Hobler [5] and developed by Mikielewicz et al. [6-7] for respectively a film flow down an inclined plane and a sheared liquid film. These authors assume semi cylindrical rivulets, with a one dimensional velocity distribution. Later, other authors developed more sophisticated models in which the 2D velocity distribution across the rivulet cross section is computed numerically, and the rivulet shape is calculated explicitly instead of making assumption on its shape. Lima da Silva et al. [3] adopted the simple approach of Mikielewicz et al. [7] for the implementation of the rivulet model in their anti-icing code.

The MTE criteria consists in a system of 4 equations with 4 unknowns: the critical film thickness for transition h_0, the rivulet radius R, the center to center rivulet spacing λ and the rivulet wetness factor F_r. As illustrated in Fig. 1. the later is a wetted area factor defined as the ratio between the rivulet base width and the spacing between two rivulets:

$$F_r = \frac{2R\sin\theta_0}{\lambda} \qquad (1)$$

where θ_0 is the contact angle along the rivulet.

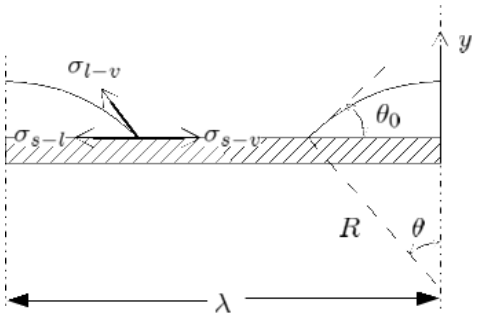

Fig. 1: Cross section of rivulets.

The set of equations to be solved consists in the mass conservation between film and rivulet flow in the streamwise direction, the conservation of total energy ($e_T = e_K + e_S$) from film to rivulet, rivulet total energy minimization and geometrical relationships. Assuming a Couette flow velocity profile $v = v(y)$, the mass flow rate per unit width in the film m'_f and rivulets m'_r is estimated by:

$$\frac{\dot{m}_f}{\lambda} = \dot{m}'_f = \int_0^{h_0} \rho v(y)dy = \frac{\rho\tau}{2\mu}h_0^2 \qquad (2)$$

$$\frac{\dot{m}_r}{\lambda} = \dot{m}'_r = \frac{2}{\lambda}\int_0^{R\sin\theta_0}\int_0^{h(x)} \rho v(x,y)dxdy = \frac{\rho\tau}{\mu}\frac{\phi(\theta_0)}{\lambda}R^3 \qquad (3)$$

where τ tis the shear stress at the film interface, ϕ and g are functions of θ_0 (see [3] for their complete expression). The total mechanical energy of the film e_f and of rivulets e_r is given by:

$$\frac{E_f}{\lambda} = e_f = \int_0^{h_0}\frac{\rho}{2}v^2(y)dy + \sigma_{lv} + \sigma_{ls} = \frac{\rho\tau^2}{6\mu^2}h_0^3 + \sigma_{lv} + \sigma_{ls} \qquad (4)$$

$$\frac{E_r}{\lambda} = e_r = \frac{\rho}{\lambda}\int_0^{R\sin\theta_0}\int_0^{h(x)} v^2(x,y)dxdy + \left(\frac{2R\theta_0}{\lambda} + \cos\theta_0 - \frac{R\sin 2\theta_0}{\lambda}\right)\sigma_{lv} + \sigma_{ls} = \qquad (5)$$

$$\frac{\rho\tau^2}{6\mu^2}g(\theta_0)h_0^3\left(\frac{\sin\theta_0}{\phi(\theta_0)}\right)^{3/2}F_r^{-1/2} + \left(F_r\frac{\theta_0}{\sin\theta_0} + \cos\theta_0 - F_r\cos\theta_0\right)\sigma_{lv} + \sigma_{ls}$$

Applying mass and energy conservation, we get the following two equations:

$$R = h_0\left(\frac{\sin\theta_0}{\phi(\theta_0)F_r}\right)^{1/2} \qquad (6)$$

$$h^+ g(\theta_0)\left(\frac{\sin\theta_0}{\phi(\theta_0)}\right)^{3/2}F_r^{-1/2} + \left(\frac{\theta_0}{\sin\theta_0} - \cos\theta_0\right)F_r - (1-\cos\theta_0) - h^+ = 0 \qquad (7)$$

The most stable rivulet pattern is found by minimizing the rivulet total energy with respect to the wetness factor:

$$\frac{\partial e_r}{\partial F_r} = 0 \text{ and } \frac{\partial^2 e_r}{\partial F_r^2} > 0 \qquad (8)$$

Combining equations (7) and (8), an equation in terms of adimensional film thickness $h^+ = \frac{\rho\tau^2 h_0^3}{6\mu^2\sigma_{lv}}$ is found:

$$h^+ = 3\times 2^{-2/3}\cdot\left(\frac{\theta_0}{\sin\theta_0} - \cos\theta_0\right)^{1/3}\cdot\left[h^+\cdot g(\theta_0)\right]^{2/3}\cdot\frac{\sin\theta_0}{\phi(\theta_0)} - (1-\cos\theta_0) \qquad (9)$$

Once h^+ is known, h_0 and F_{r0} can be easily deduced, as well as λ and R.

3. CFD simulations of the airflow

As underlined before, one input of the MTE model is the shear stress distribution on the liquid film, which is approximated here by the distribution around the airfoil in single phase conditions. For that purpose, several computations are performed around a NACA0012 airfoil with zero angle of attack and for Reynolds numbers ranging between $Re_c = 0.67\cdot 10^5 - 1.69\cdot 10^5$, reproducing the experimental conditions of Zhang et al. [4]. The simulations are run with the finite volume code OpenFoam.

Beforehand, the solver was validated for a NACA0012 test case at zero angle of attack, and Reynolds number $Re_c = 6\cdot 10^6$, for which experimental and numerical data is provided by NASA [8]. Structured hexahedral C-type

meshes are used, with respectively 146,000 and 443,000 cells. In order to solve the boundary layer, the first cell height normal to the wall is set at $y = 4 \cdot 10^{-6}$ m, ensuring $y^+ < 1$. The SIMPLE algorithm is used, while a second order upwind scheme is chosen for convective term discretization and limited second order central scheme for the diffusion term. Turbulence is accounted for with a k-ω SST model. The distribution of friction coefficient C_f is confronted in Fig.2 to the reference numerical data provided in [8] and obtained with a NASA solver CFL3D k-ω SST. The agreement is excellent, supported by a predicted drag coefficient of $C_D = 0.00805$ very close to the experimental value $C_D = 0.0083$ of Ladson et al. [9]. It is concluded that the $k\omega - SST$ model implemented in OpenFoam 2.3 can be used with confidence for the computations corresponding to Kai's experimental data, with a chord length $c = 0.101m$. A similar set-up was used for the simulations, although it is important to underline that Zhang´s experiments [4] were performed at $Re_c = 0.67 \cdot 10^5 - 1.69 \cdot 10^5$, hence laminar conditions are expected along almost all the chord. This is why the transition model $kkL - \omega$ of Keith [10] is also used here. Nevertheless, the presence of the water film which undergoes surface shear instabilities is probably sufficient to trip turbulence near the leading edge. This justifies the use of the fully turbulent model $k\omega - SST$. The friction coefficient distributions obtained at $R_e = 1.69 \cdot 10^5$with the two turbulence models are plotted in Fig.3, for two meshes of 117,000 ($y^+ \sim 1$) and 235,000 cells ($y^+ < 1$) respectively. Starting from *x/c*=0.15, we can clearly see the deviation between the $k\omega - SST$ predictions, which are turbulent and attached all along the foil, and the $kkL - \omega$ predictions which show flow separation and transition near the trailing edge, at *x/c*=0.9. It can be anticipated that the discrepancy between the two models on the first half of the chord will have a non negligible influence on the MTE model because according to Zhang et al. [4], transition to rivulets takes place between *x/c*=0.2 and 0.4. It is difficult to assess with certainty the boundary layer regime along the foil in those particular conditions.

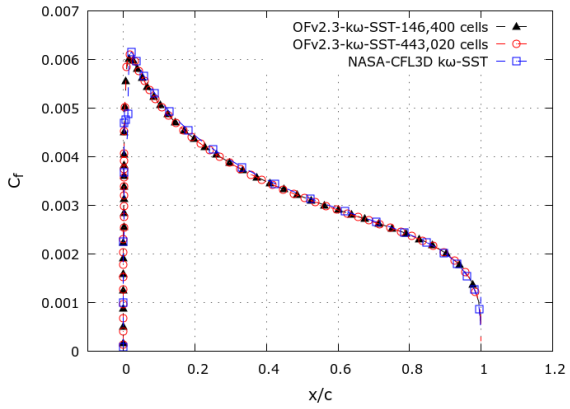

Fig. 2. NACA0012 validation test case at $Re_c = 6 \cdot 10^6$

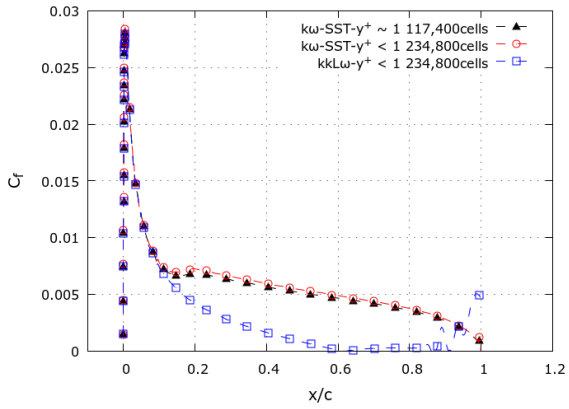

Fig. 3.Test case of Zhang etal.[4] at α*=0° and* $Re_c = 1.69 \cdot 10^5$

4. Model validation

The shear stress distributions with the $k\omega - SST$and $kkL - \omega$ models are now injected in equation (9) to predict the critical film thickness h_0 and the rivulet spacing λ for a water film of surface tension σ=0.07 N/m. Since the contact angle of the rivulet is not given in [4], it is varied between 30 and 60 ° to study the sensitivity of the model to this parameter. In Fig.4, the critical film thickness below which transition should occur is represented as a function of the position *x/c* along the chord. On the same graph, the mean thickness distribution measured by Zhang et al. [4] is plotted together with the uncertainty of the measurements estimated at ±20µm.

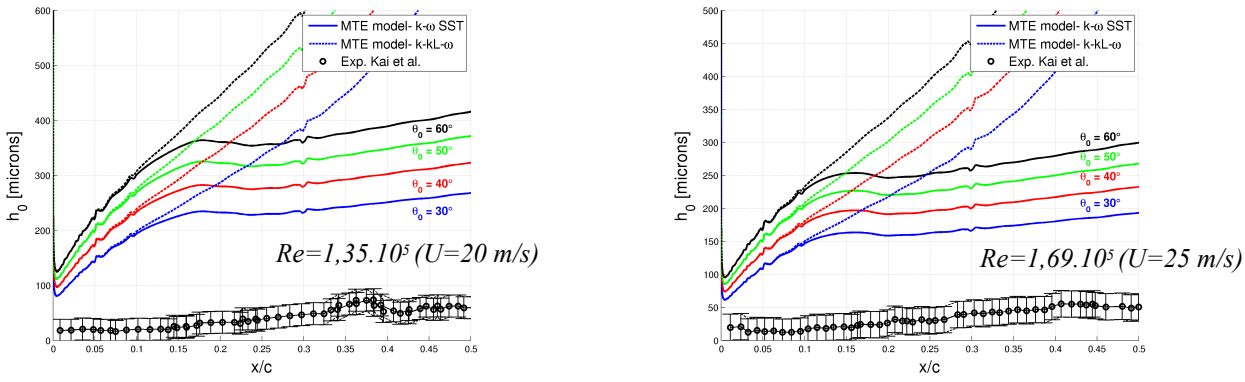

Fig. 4: Critical film thickness h_0 *predicted by the MTE model.*

At two different Reynolds numbers, it turns out that the measured thickness is well below the predicted h_0, which means that transition to rivulets should be immediate. In the experiments of Zhang et al. [4], it seems the film is continuous due to the non stop impingement of droplets near the leading edge. In addition, the average thickness in this region reaches the order of magnitude of the uncertainty. In their anti-icing code, Lima da Silva et al. [3] consider that even if the critical thickness is reached inside the impingement region, the film does not break down into rivulets due to the effects of multiple droplet impact and spreading. Similarly, transition to rivulets in the predictions of Al-Khalil et al. [2] is immediate out of the impingement limits. Therefore, it is not inconsistent to predict critical thicknesses lower than the actual values, especially not knowing where the impingement limits of the sprays are located.

The optimum rivulet spacing λ is then confronted to the experimental findings of Zhang et al. [4] in Fig 5. The mean spacing is estimated through digital image processing of the time averaged thickness mappings provided by Zhang et al. A sample image for each condition is added in Fig.5. The uncertainty is approximated by the standard deviation of the measurements. For both Reynolds numbers, it is found that the experimental points fall within the uncertainty of the predictions, due mainly to the contact angle and boundary layer regime. The order of magnitude of λ is reasonably well predicted, but there remains unknowns to prove the validity of the MTE model on an airfoil. The process of transition to rivulets is probably different from the one that occurs when a film is thinning, and the influence of droplet impingement cannot be neglected.

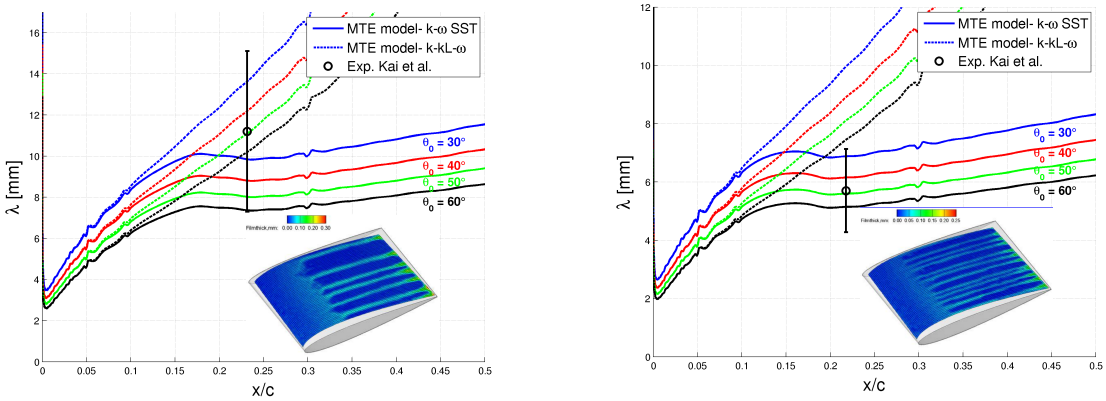

Re=1,35.10⁵ (U=20 m/s) *Re=1,69.10⁵ (U=25 m/s)*

Fig. 5: Rivulet spacing λ predicted by the MTE model.

Conclusions

The Minimum Total Energy criteria is applied to predict transition to rivulets on a sheared liquid film on an airfoil. Due to its simplicity, this model has been used in anti-icing codes but it is the first time that it is validated in isothermal conditions. The critical thickness for transition along the foil is found to be well above the experimental data of Kai et al., which makes us think that in fact, transition to rivulets occurs right after the impingement limits. The rivulet spacing at the location of transition is reasonably well predicted, but there remains some doubts about the boundary layer regime on the foil. For ice accretion applications, it seems therefore unrealistic to discard the process of generation of the liquid film. In the next future, we plan to perform simulations with an OpenFoam solver that computes droplet impingement and film formation on a solid surface, and features treatments for partial wetting phenomena in order to account for the behavior near the contact-line.

The financial support of Universidade da Coruña for the stay at Onera is gratefully acknowledged.

References

1. Diez J. and Kondic L., *Phys. Rev. Lett.* **86(4)**, 632-635 (2001).
2. Al-Khalil K., Keith, T., de Witt K., 5th Symp. Numerical and Physical aspects of Aerodynamic Flows (1992).
3. Lima da Silva G., Mattos Silvares O., Zerbini E., 9th AIAA Joint Thermophysics and Heat Transfer Conference (2006).
4. Zhang K., Johnson B., Rothmayer A., Hu H., 52th Aerospace Sciences Meeting (2014).
5. Hobler T., *Chemia Stosow* **2B(201)** (1965).
6. Mikielewicz J., Moszynski J. R., *Int. J. Heat Mass Transfer* **19**, 771-776 (1976).
7. Mikielewicz J., Moszynski J. R., *Polzka Akademia Nauk. - Prace Instytutu Maszyn Przeplywowych* **66**, 3-11 (1975).
8. NASA, Turbulence Model Benchmarking Working Group(TMBWG) , http://turbmodels.larc.nasa.gov/naca0012_val.html
9. Ladson, C. L., Hill, A. S., and Johnson, Jr., W. G., NASA TM 100526 (1987).
10. Keith Walters, D., Cokljat, D., *J. Fluids Engineering* **130**, 121401 (2008).